PHOTONICS Research

Refocusing of the optical branched flow on a rough curved surface

Weifeng Ding, Zhaoying Wang,* and Chaokai Yang

Zhejiang Province Key Laboratory of Quantum Technology and Device, School of Physics, Zhejiang University, Hangzhou 310027, China
**Corresponding author: zhaoyingwang@zju.edu.cn*

Received 3 August 2023; revised 12 September 2023; accepted 12 September 2023; posted 12 September 2023 (Doc. ID 502521); published 22 November 2023

The phenomenon of branched flow has attracted researchers since its inception, with recent observations of the light branching on soap bubbles. However, previous studies have primarily focused on the flat spacetime, overlooking the effect of surface curvature on branched flows. In this paper, we explore the branched flow phenomenon of light on a rough curved surface called constant Gaussian curvature surfaces (CGCSs). Compared with flat space, a CGCS demonstrates that the first branching point advances due to the focusing effect of the positive curvature of the surface. Furthermore, unlike on flat space, optical branches on curved surfaces do not consistently become chaotic during its transmission in a random potential field. On the contrary, the "entropy" decreases at specific positions, which reveals a sink flow phenomenon following the generation of branched flows. This result highlights the time inversion characteristics of CGCSs. Lastly, we demonstrated that the anomalous entropy reduction is related to the transverse and longitudinal coherence transformations of light. We suppose these efforts would fuel further investigation of the thermodynamic evolution and spatiotemporal inversion of random caustics, as well as their future application in the information transmission of random potentials in curved spacetime.

https://doi.org/10.1364/PRJ.502521

1. INTRODUCTION

A fascinating phenomenon called branched flow occurs when a wave passes through a weak disordered potential whose relative length exceeds its wavelength. The gradual variation in disorder produces focused, elongated filaments that branch out, forming tree-like structures rather than random speckle patterns. This branched flow appears to be irreversible, from the trunk to the branch, and originates from the ray deflections due to weakly correlated changes in potential, leading to the formation of caustics [1]. These caustics reflect the folding of the Lagrangian manifolds in phase space, which corresponds to the concentration of rays and high field strengths along specific lines on 2D or 3D surfaces [2]. When initially observed in electrons [3–7] and microwave cavities [8,9], branched flow is thought to occur across a broad spectrum of wavelengths. In fact, branched flows are believed to play a pivotal role in focusing ocean waves [10,11]. In the case of light, however, this phenomenon has only recently been subtly observed on soap bubbles [12].

An interesting but easily overlooked point is that the branched flow phenomenon has a time arrow. Because of the existence of the random potential field, the time inversion symmetry of the Helmholtz equation is broken, and the optical path loses reversibility. In the intuitive physical picture, when we consider the inversion of time, the branched waves within these filamentous structures refocus to create robust trunks [13]. This counterintuitive process seems to violate the principle of entropy increase, which dictates a natural tendency towards chaos. Yet on curved surfaces, specifically those with constant Gaussian curvature surfaces (CGCSs), it is possible to achieve this effect to some extent, thanks to the periodic properties of light transmission. The general theory of relativity offers rich potential for studying electromagnetic waves in curved spacetime, where two-dimensional surfaces are often used as laboratory simulations of the effects of gravitational fields [14]. In addition to advances in geometric optics, such as gravitational lensing [15], more interesting effects were discovered, such as the relativistic Hall effect [16,17], the Wolf effect [18,19], and chaotic [20] and wave redirection [21]. Among them, the electromagnetic wave equation on the curved surface established by Batz and Peschel [22] has become a key tool. They predicted that the coherent electromagnetic wave transmission on the CGCS has periodic properties, and in one period, the second half period can be regarded as the time inversion of the first half period, which can also be obtained by the matrix optical method [23,24]. This gives us a scheme to achieve the temporal inversion of branched flow phenomena.

In recent experiments with optical branching flows on soap bubbles [12], the bubbles they studied were large enough to consider flat, smooth thickness variations in the film acting as a correlated disordered potential. They verified that the distance from the launch point to the first branching point leads to a scaling law that depends upon the optical potential strength and its correlation length. In this paper, we propose that this relationship on the curved surface should be corrected by the curvature of the surface and can be described by the scintillation index ($S_c I$) [25]. The $S_c I$ is one important parameter for describing the appearance of branches, as they periodically become abnormally larger, which is caused by the optical sink flow of the surfaces.

The magical sink flow on the curved surface is a phenomenon of reverse branched flow, which is a process from disorder to order. Following the concept of thermodynamics, we define a new index called "branched flow entropy," and prove that the entropy increase principle is temporarily broken in the inverse branch flow on a curved surface. The degree of entropy reduction is closely related to the curvature of the surface and the parameters of the random potential field. Further, we explore that this is because the decoherence process is blocked by the curved surface, and the decreasing coherence of the light will rise periodically, which gives us inspiration for studying the influence of spatial structures on the conservation of information. In addition, since the CGCSs are often used to simulate curved spacetime with uniform mass densities, the Friedmann–Robertson–Walker (FRW) metric, our research can also be extended to the cosmology [26]. Considering that macroscopic surfaces can be approximately flat, the refocusing phenomenon of branched flow on curved surfaces will be more significant at microscopic levels, such as in droplets [27] or biological cells [28]. Therefore, microscopic particle size analysis may be one of the possible applications of this research. Additionally, this research could use extremely intense lasers or electron streams [29,30], which could help in the study of extreme radiation and field.

2. RESULTS

We begin our study of optical branched flow and the corresponding time reversal on a special type of 2D curved surface in 3D space, CGCS, by investigating the plane wave and the Gaussian beam propagation on the rough curved surfaces with random fluctuations. The CGCS has revealed various properties on which light is transmitted, such as periodic convergence and divergence of the light spot and oscillation of the transmission trajectory [26,31,32]. By convention, we define the coordinate system, as shown in Fig. 1(a), where ρ is the equatorial, and h is the arc length of the generating line (longitude and latitude). The light transporting on a two-dimensional curved surface can be described by the scalar Helmholtz equation [33],

$$(\Delta_g + k^2)\Psi + (H^2 - K)\Psi = 0,$$

where H stands for average curvature, while K stands for Gaussian curvature. It has been proved that the effect of the average curvature H is negligible when the wavelength of the light wave is small, i.e., our rough surface can be considered as follows: $H \sim 0$, $K' = K + \Delta K(h, \rho)$, where K is a constant and ΔK is the curvature fluctuation depending on the position of the curved surface.

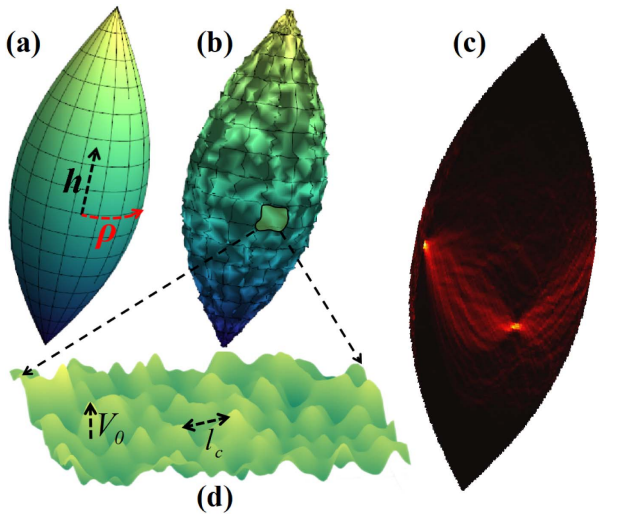

Fig. 1. CGCS images with positive Gaussian curvature. (a) Smooth and (b) rough. (c) Light beam transmits on the rough CGCS. (d) Local rough surface.

It has been known in previous discussions, namely [32], that the effect of the curvature on the CGCS in the paraxial approximation can be equivalent to a second-order potential field $V_{\text{eff}} = 1 - Kh^2$, and the Helmholtz equation with paraxial approximation on a CGCS can be written as

$$2ik\partial_\rho u = -Kr^2\partial_h^2 u + (V_{\text{eff}} + V_R)u. \quad (1)$$

This is similar to the Schrodinger equation, where we divide the potential field into two parts: the harmonic oscillator potential due to a curved surface, and the random potential due to the surface roughness (the undulation of the surface), shown as Fig. 1(b). The curvature changes caused by rough fluctuations can be separated into V_{eff} and V_R in the Helmholtz equation under the weak field approximation. The roughness of a surface can be described by the random potential of the Gaussian correlation with the correlation length l_c [1,34],

$$\langle V(r)V(r')\rangle = V_0^2 e^{-|r-r'|^2/l_c^2}, \quad (2)$$

where V_0 is the amplitude of the random potential field [see Fig. 1(d)]. Rather, in simulation, we find that the conditions must be restructured to enable fluctuation in the proper range. Otherwise, the light patterns would be wave-guiding channels with a higher effective refractive index. Alternatively, it could be a nonlinear process such as surface polariton production [35]. Another possibility is that the light is guided by the membrane's deformation due to optical forces [36].

The generatrix equation of CGCS is $R = R_0 \cos(\sqrt{K}h)$, where the relationship between R_0 and K determines the shape. In particular, $KR_0 = 1$ is spherical, and we take the olive shape of $KR_0 = 1/2$ as the light transport surface for our paper. In our simulation, as shown in Fig. 1(d), the branched flow of light also appears on the curved surface, but then, time inversion occurs, and other abnormal peaks in the $S_c I$ appear. The $S_c I$ is used to describe the normalized variance of the branched flow intensity,

$$S_cI(\rho) = \frac{\langle I^2(\rho, h)\rangle}{\langle I(\rho, h)\rangle^2} - 1. \quad (3)$$

We can visually understand that the distribution of light intensity is denser in the position with a larger scintillation index. After the maximum point of S_cI, the degree of light convergence begins to decrease.

Based on Eq. (1), in a random potential field with Gaussian correlation, the evolutions of light transmission on a flat surface and on a CGCS are demonstrated, as shown in Figs. 2(a)–2(d), by using the method of fast Fourier transform. In our simulation, according to Ref. [12], the beam size of the Gaussian light is set as 20 μm, and the wavelength of the light is set as 500 nm. The correlation length of 100–300 μm is performed in the calculation, which is approximately hundreds of times the wavelength and 10 times the size of the Gaussian spot. For convenience, we set all the calculation parameters to be dimensionless in the following. The white line shows the change of the S_cI of the plane waves with transmission. The highest point of the S_cI corresponds to the first branching position d_0 of the light beam, and it obeys the scaling law as the distance to the first caustic position $d_0 \sim l_c V_0^{-2/3}$ when the light travels in flat space [1,9], as shown on the dark point of the black curve in Fig. 2(e). We also find that the first caustic position on the curved surface appears earlier than that on the flat surface. Furthermore, as the curvature K increases or the amplitude of the random potential field increases, the branching position will be more advanced, as shown in Figs. 2(e) and 2(f). This advance is closely related to the focusing effect of the positive curvature surface on the light, which shortens the effective transmission distance of the light and speeds up the branching process. In Fig. 2(f), the fitted lines represent a proportional relationship between the curvature K and the first focus position d_0. For Gaussian beams, this branch position advance phenomenon also appears on the curved surface. But because the initial scintillation index of Gaussian light is large, it is difficult

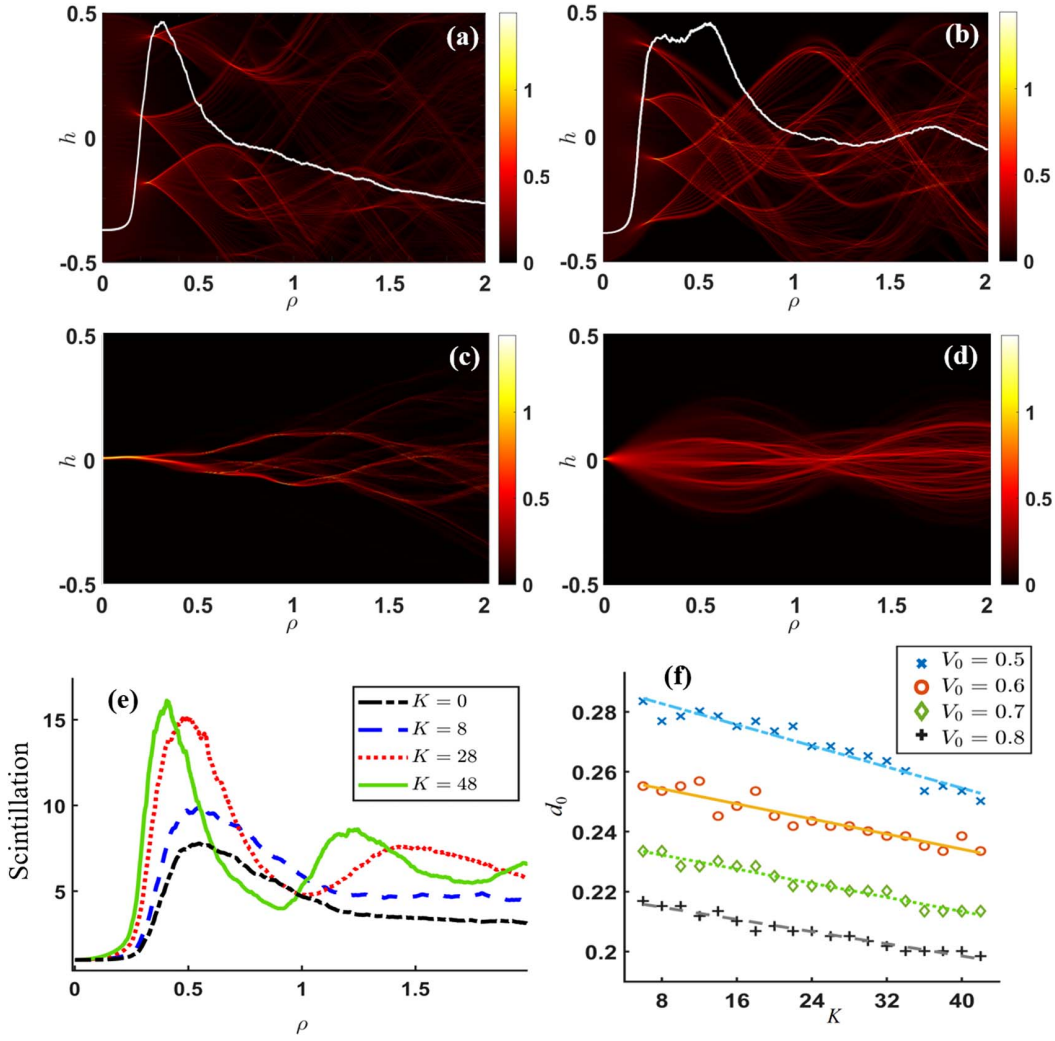

Fig. 2. Beam is transmitting in a Gaussian correlated random potential. (a) and (b) are the plane waves propagating on a flat surface and a CGCS, respectively, and the white line is the evolution of the S_cI with light transmission. (c) and (d) are the Gaussian light propagating on flat surfaces and CGCSs, respectively. (e) Change of the S_cI of the plane waves on the CGCS with different curvatures. (f) The position of the first branching point of plane wave varies with the curvature of the curved surface and the magnitude of the random potential field V_0.

to identify the position of the first peak; here, we only show the $S_c I$ changes with the transmission distance of the plane waves.

In addition, in Fig. 2(e), when the curvature of the surface increases to a certain value, two or more peaks of $S_c I$ will appear. The presence of the remaining peaks indicates that the light field has an anomalous flare after branching. We discover that the first peak is at the location where the branched flow is generated, while the second peak corresponds to a special convergence position of the light on the curved surface.

This similar phenomenon can happen to the Gaussian beam. Figure 3(a) presents the evolution of the Gaussian beam in the random field on the CGCS. The size of the main peak of the waveform will first expand and then converge. As shown in Figs. 3(b) and 3(c), a single-peak Gaussian light changes into multiple branches and then returns to one main peak with multiple secondary peaks, meanwhile the maximum light intensity decreases first and then increases, although the intensity of the main peak cannot return to the original value.

During the propagation, the branched flow process of light is partially reversed, and the scattered branches of light flow converge again, becoming more orderly, which is known as sink flow. This interesting phenomenon indicates that when light travels on a curved surface, its disorder does not always increase, but it may cause anomalous changes at some positions. In order to better explain this phenomenon, we introduce a concept similar to thermodynamic entropy to describe the chaos degree of light rays. Referring to the concept of thermodynamics, we define the entropy of branched flow as the following expression to describe the chaos of the light beam:

$$S_{\mathrm{bf}} = -\sum P(I) \ln P(I), \tag{4}$$

where $P(I)$ represents the probability density distribution of the light intensity. In the initial position, the plane waves are used for simulation, and the distribution of the light intensity satisfies the delta function $P(I) = \delta(I - I_0)$ theoretically,

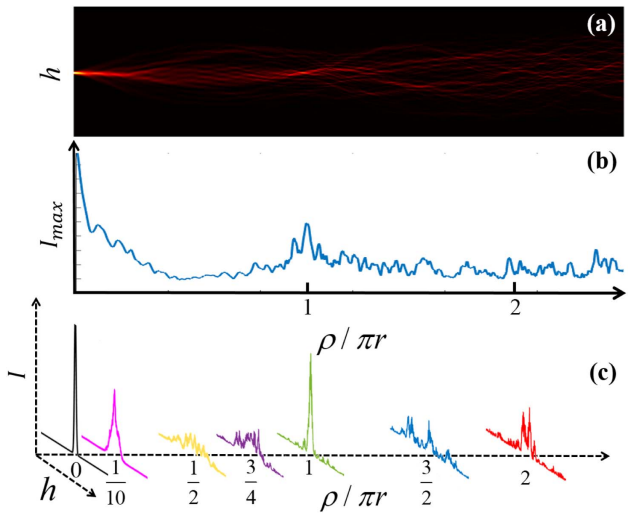

Fig. 3. (a) Evolution of the Gaussian beams in random fields on the CGCS. (b) Change of the maximum intensity of light with respect to transmission. (c) Evolution of the transverse light intensity distribution.

as shown in panel (P1) of Fig. 4(a). From Fig. 4(a), the entropy on the CGCS increases like that on a flat surface at the beginning of transmission. However, after transmission for a certain distance, a temporary decrease of the entropy occurs, and a small "pit" appears on the transmission-dependent entropy curve. During this transmission process, the probability density distribution changes from exponential [panel (P2) in Fig. 4(a)] to a Gaussian-like distribution [panel (P3) in Fig. 4(a)], and becomes exponential [panel (P4) in Fig. 4(a)] again. Figures 4(b) and 4(c) show the variation of the branch-flow entropy in the random potential on a flat surface and a CGCS, respectively. The correlation length of the random potential field affects the evolution of entropy at the beginning of transmission but tends to a same value at the end. On the curved surface, during the beam transmission, there are two or more processes of entropy reduction due to the convergence of the branched flow.

3. DISCUSSION

In flat space, when an electromagnetic wave travels in a random medium over a long distance, the light intensity is a strong fluctuating quantity, which is classically described by Rayleigh statistics. The distribution function $P(I)$ is a negative exponential [37],

$$P(I) = \frac{1}{\langle I \rangle} \exp\left(-\frac{I}{\langle I \rangle}\right). \tag{5}$$

However, the Rayleigh distribution only applies to the completely coherent light, while the partially coherent light has a coherence-dependent probability distribution of light intensity in the random medium [38]. The influence of $P(I)$ caused by the change of coherence degree is very similar to that of the random potential field with the change of transmission distance. For example, the log-normal distribution appears at the position of entropy reduction [see Fig. 4(a)], which is similar to the situation of partially coherent light. So, in our paper, we believe that the evolution of the energy distribution along with the transmission is also closely related to the coherence degree, $\alpha = |\langle E \rangle^2| / \langle I \rangle$.

Before studying the curved surface, we can first demonstrate the influence of the random potential field on the coherence of the flat surface. By solving the Helmholtz equation numerically, the electric field and light intensity distribution of the optical branch flow are obtained. During the numerical simulation, 500 random fields with consistent parameters were generated, and the evolution of optical coherence was obtained on average. It is found that with the light transmission, the coherence can be viewed as decreasing exponentially, $\alpha = \exp(-b\rho)$, and gradually tends to 0, as shown in Fig. 5(a). The coherence attenuation factor b is related to the fluctuation V_0 and the correlation length l_c of the random potential field, as shown in Figs. 5(b) and 5(c).

On the curved surface, as long as the light intensity moment $\langle I^n \rangle$ is expanded (see Appendix A), the evolution of light intensity distribution can be naturally obtained. Then, the relationship between the intensity distribution of the partially coherent light and the coherence degree after multiple scattering by random mediums will take the following form [8]:

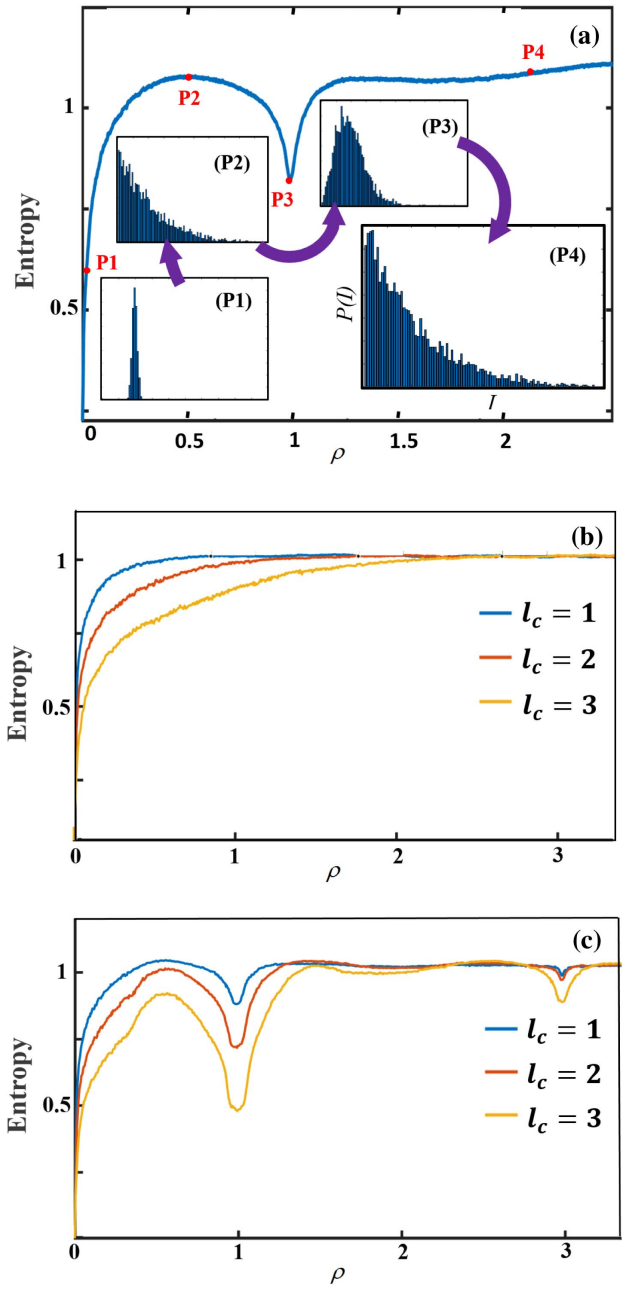

Fig. 4. (a) Evolution of the entropy of the optical branched flow when it transmits on a curved surface. (P1)–(P4) Light intensity probability distribution. For the different correlation lengths, the branched flow entropy of the beam varies with the transmission on (b) the flat surface and (c) the CGCS.

$$P(I) = \int_{-\infty}^{\infty} \exp(i\xi I) \frac{\exp\left(-\frac{i\xi\alpha}{1+i\xi(1-\alpha)}\right)}{1 + i\xi(1-\alpha)} \frac{\mathrm{d}\xi}{2\pi}, \tag{6}$$

where ξ is an integral constant. We can substitute the exponential decreasing relation of the flat space into Eq. (6). Then, we can calculate the theoretical evolution of this $P(I)$ with the transmission ρ, as shown in Fig. 5(g), which is close to our simulation results [panels (P1)–(P4) in Fig. 4(a)]. In fact, Figs. 4(a) and 5(g) describe the situation of the curved surface and the flat surface, respectively. Due to the entropy increasing on the flat surface while the possible entropy reduces on the curved surface, the transmission distance ρ in Fig. 5(g) cannot be directly compared with that in Fig. 4(a). The transverse coherence of light decreases in random fields for both the flat space [Fig. 5(a)] and the CGCS [Fig. 5(e)], but the decrease is oscillatory in the CGCS. Thus, on the curved surface, the decoherence process induced by random medium scattering is reciprocating but not monotonous. The weakening of the "connection" between photons is actually the reason for the entropy increase, while the unique function of the fractional Fourier transformation on the CGCS [39] establishes new connections between photons, resulting in a temporary decrease of entropy. Quantitatively, if we consider the case of separable variables, then the coherence factor can be written as $\alpha = f(K,\rho)\exp(-b\rho)$. Unlike the flat surface, here the amplitude factor f depends on the curvature of the curved surface.

From Figs. 5(b) and 5(c), b is proportional to the square of V_0 while the variation of b with l_c is a logarithmic Gaussian distribution. The coherence of the optical branched flow will decrease with the increasing V_0, which leads to the acceleration of the entropy increase process. In addition, on a curved surface, an increase of V_0 will weaken the entropy reduction effect and even make it disappear. Furthermore, from Fig. 5(f), it is found that the position of the first peak in the curve of Fig. 5(e) is positive with the reciprocal of the curvature. Through the synthesis of the above numerical relations, we can deduce an analytic expression,

$$\alpha = J_0(p_1 K\rho)^2 \exp(-b(l_c, V_0)\rho), \tag{7}$$

where $b = V_0^2 \exp(-p_2(\ln l_c - p_3)^2)$ and $p_{1,2,3}$ are the optical parameters independent of the potential field and spacetime background. When substituting Eq. (7) into the calculation of entropy, we find that it is the coherence of light that leads to a periodic decrease of entropy, although the amplitude is small and only lasts for a few periods, as shown Fig. 5(d).

In particular, the CGCS can be regarded as a rotation in phase space composed of the momentum and position of the light. What we calculated above is the spatial coherence (transverse coherence). At the same time, the CGCS will also become such a transformation system, which periodically converts the temporal coherence (longitudinal coherence) into the spatial coherence, resulting in a brief reversal of the decoherence process. In fact, the reduction of temporal coherence has been reported in other literature, e.g., the so-called Wolf effect [19]. It shows that the curved spaces with larger positive curvature accelerate and enhance the spectral shifts (blue shifts or red shifts) of light during their propagation.

It is worth emphasizing that in this study we do not have a clear delineation of the material that constitutes the curved surface. The optofluidic system can be formed by the optical branched flow with liquid surfaces, such as soap bubbles mentioned in the literature [12], biological cells, and even the ocean. It can also be formed with solid structures such as nanostructure, fiber, or metasurface. In optofluidic systems, there are some examples that can be further considered, such as the optical control of the thermocapillary effects [40], stochastic solitons, or occurrence of turbulence at low Reynolds numbers. Applications to solid systems include particle manipulation

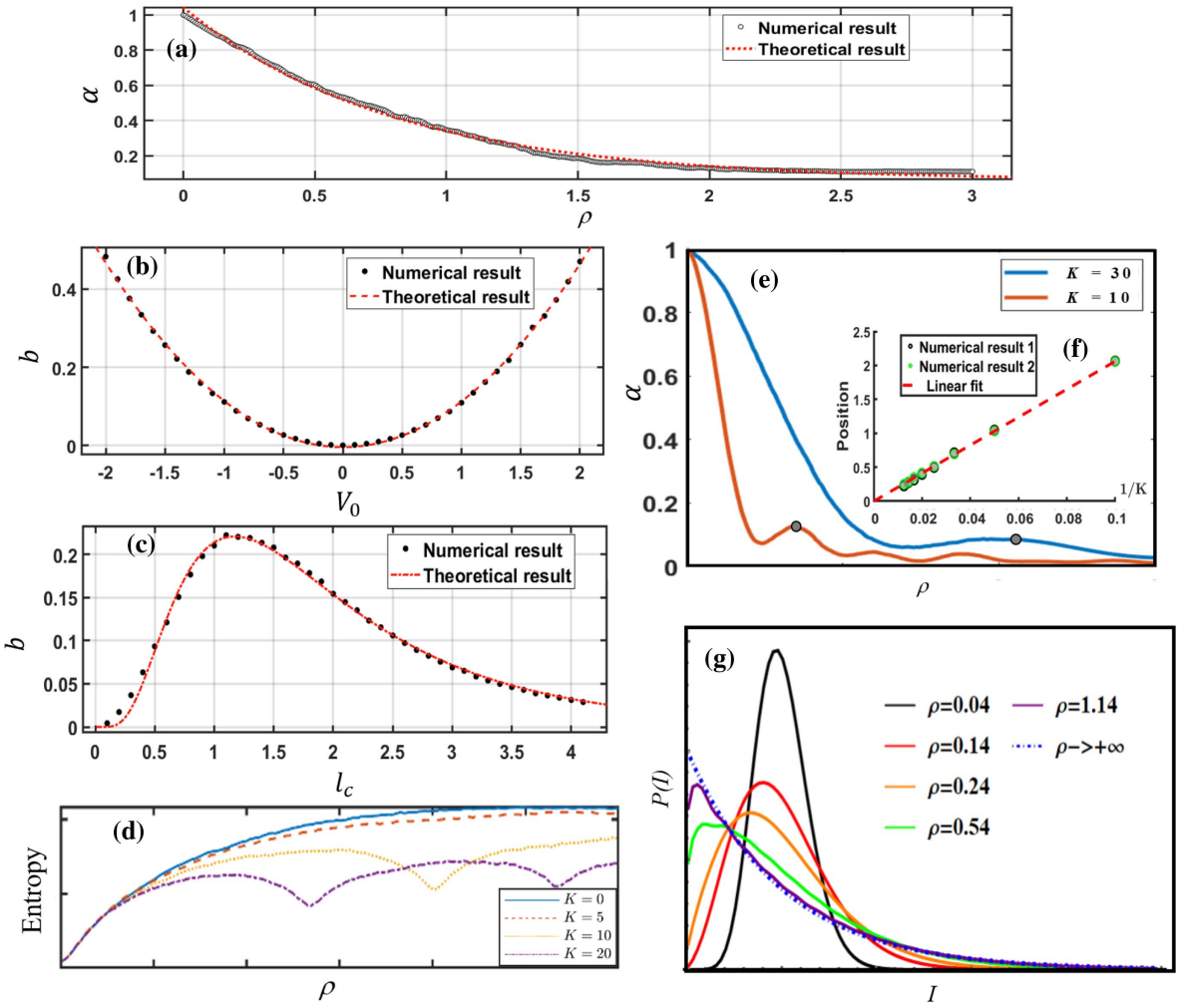

Fig. 5. (a) Evolution of the coherence degree of the branched flow with transmission on a flat surface. (b) and (c) are the relationship between the attenuation factor b and the random potential field parameters V_0 and l_c, respectively. (d) Theoretical evolution of branching flow entropy under different curvatures. (e) Evolution of the coherence degree of the branched flow on curved surfaces with different curvatures. (f) Change of the position of its first peak in the curve of (e) with different curvature. (g) Theoretical evolution of the probability distribution of the light intensity with different ρ on a flat surface.

[41], random scattering quasi-two-dimensional resonator [8], and so on. The universality of the discussion in this paper means that it is not related to the constituent matter but only to the curvature of the surface. This is reminiscent of the same "hairless" black hole, so we cannot help but ask whether the entropy reduction here has the same deeper roots as Bekenstein entropy [42], and how the entropy reduction relates to the thermodynamic effects of the event horizon.

4. CONCLUSION

In conclusion, we have investigated the phenomenon of optical branched flow on a CGCS. The CGCS is rough, with a random slight fluctuation potential field, which satisfies both the generation condition of the branched flow and the weak field approximation. In the case of paraxial transmission, the first branching position of the optical branched flow on the CGCS is earlier than that on the flat surface, which shows that the focusing characteristic of the positive curvature surface shortens the length of the wave caustics. On the curved surface, there is a phenomenon of anti-branched flow, called sink flow, which is impossible to appear on the flat surface. Through simulations, we found that the "branched flow entropy" near the sink flow point decreases temporarily with the transmission, indicating that the optical intensity distribution becomes ordered at this location.

In the discussion, we demonstrated that the entropy reduction is closely related to the coherence of the optical field, and the increase of the curvature of the surface will accelerate the conversion from the longitudinal coherence to the transverse to resist the decoherence of the light caused by the random field. Moreover, the effects of the random field and the surface parameters on the evolution of the optical coherence were studied. Based on this, we deduced a theoretical expression of entropy reduction, which agrees with the simulation results.

We obtained this time reversal of branched flow because of the unique focusing property of the CGCS, which is a nonlocal effect. In fact, if we consider the transmission of branched flow on surfaces with slowly changing curvature, this inversion property is also possible, but much worse than that of the CGCS. If the optical branches propagate on the CGCS with negative curvature for the location of the scintillation index and the first branching point of the branched flow, compared to the flat surface, then the negative curvature surface will have a hysteresis effect, which is the opposite of the CGCS with the positive curvature. Furthermore, our simulation showed that CGCS with negative curvature will lose the temporary entropy reduction effect of the optical branched flow, and the time inversion phenomenon will disappear simultaneously. The entropy reduction, which is monitored by the curvature of the surface and roughness parameters, can be used to enlighten multi-mode fiber amplifiers to improve pump absorption efficiency under complex backgrounds with nonuniform transverses [43,44]. The research can also be extended to other types of wave transport on curved surfaces, such as the transmission of ocean currents branching on the Earth's surface [11]. In addition, according to Einstein, gravitational fields can be thought of as curved spacetime. The exploration of branched flow and entropy within the context of non-Euclidean geometry may give a new perspective in the study of conservation of information and chaos in cosmology.

APPENDIX A: PROOF OF THE RELATION BETWEEN INTENSITY PROBABILITY DISTRIBUTION AND COHERENCE DEGREE

Because of the completeness of the exponential family of distributions, we can write $P(I)$ for different evolutionary processes or different coherence degrees as follows. This is physically equivalent to a superposition of a heat distribution with a certain temperature distribution width,

$$P(I) = \sum_i g_i P_{Ri}(I_i). \tag{A1}$$

Each of these individual sub-distribution P_{Ri} is a Rayleigh distribution. So, at this point, we can simply get the n-order moment of light intensity, which will satisfy $\langle I^n\rangle = \int I^n \times P(I)\mathrm{d}I = n!\langle I\rangle^n$ because of the derivative property of the exponential function. We expand the light intensity to the power n by binomials as follows:

$$\begin{aligned}\langle I^n\rangle &= n!\langle I\rangle^n = n!(\langle I\rangle - |\langle E\rangle^2| + |\langle E\rangle^2|)^n \\ &= \sum_{m=0}^{n} C(m,n)|\langle E\rangle^2|^m(\langle I\rangle - |\langle E\rangle^2|)^{n-m},\end{aligned} \tag{A2}$$

where $C(m,n) = \frac{(n!)^2}{(m!)^2(n-m)!}$. In statistics, the distribution of a random variable can be obtained by knowing all its moments by the following formula:

$$P(I) = \int_{-\infty}^{\infty} \exp(i\xi I)\sum_n \frac{(-i\xi)^n}{n!}\langle I^n\rangle \frac{\mathrm{d}\xi}{2\pi}. \tag{A3}$$

By combining Eqs. (A2) and (A3), we get

$$\begin{aligned}P(I) = \int_{-\infty}^{\infty} \exp(i\xi I)\sum_n \frac{(-i\xi)^n}{n!}\Bigg(\sum_{m=0}^{n} C(m,n) \\ \times |\langle E\rangle^2|^m(\langle I\rangle - |\langle E\rangle^2|)^{n-m}\Bigg)\frac{\mathrm{d}\xi}{2\pi}.\end{aligned} \tag{A4}$$

Notice that Eq. (A4) is actually a Taylor expansion, and since $\frac{n!}{(n-m)!}X^{n-m} = \frac{\mathrm{d}}{\mathrm{d}X^m}X^n$ holds, we have the following formula:

$$P(I) = \int_{-\infty}^{\infty} \exp(i\xi I)\frac{\langle I\rangle \exp\left(-\frac{i\xi|\langle E\rangle^2|}{1+i\xi(\langle I\rangle - |\langle E\rangle^2|)}\right)}{\langle I\rangle + i\xi(\langle I\rangle - |\langle E\rangle^2|)}\frac{\mathrm{d}\xi}{2\pi}, \tag{A5}$$

which is consistent with Eq. (6) in the main text.

Funding. National Natural Science Foundation of China (12274366).

Disclosures. The authors declare no conflicts of interest.

Data Availability. No data were generated or analyzed in the presented research.

REFERENCES

1. L. Kaplan, "Statistics of branched flow in a weak correlated random potential," Phys. Rev. Lett. **89**, 184103 (2002).
2. Y. A. Kravtsov and Y. I. Orlov, "Caustics, catastrophes and wave fields," Sov. Phys. Usp. **26**, 1038–1058 (1983).
3. M. A. Topinka, B. J. LeRoy, R. M. Westervelt, S. E. J. Shaw, R. Fleischmann, E. J. Heller, K. D. Maranowski, and A. C. Gossard, "Coherent branched flow in a two-dimensional electron gas," Nature **410**, 183–186 (2001).
4. M. P. Jura, M. A. Topinka, L. Urban, A. Yazdani, H. Shtrikman, L. N. Pfeiffer, K. W. West, and D. Goldhaber-Gordon, "Unexpected features of branched flow through high-mobility two-dimensional electron gases," Nat. Phys. **3**, 841–845 (2007).
5. K. E. Aidala, R. E. Parrott, T. Kramer, E. J. Heller, R. M. Westervelt, M. P. Hanson, and A. C. Gossard, "Imaging magnetic focusing of coherent electron waves," Nat. Phys. **3**, 464–468 (2007).
6. D. Maryenko, F. Ospald, K. von Klitzing, J. H. Smet, J. J. Metzger, R. Fleischmann, T. Geisel, and V. Umansky, "How branching can change the conductance of ballistic semiconductor devices," Phys. Rev. B **85**, 195329 (2012).
7. B. Liu and E. J. Heller, "Stability of branched flow from a quantum point contact," Phys. Rev. Lett. **111**, 236804 (2013).
8. R. Höhmann, U. Kuhl, H. J. Stöckmann, L. Kaplan, and E. J. Heller, "Freak waves in the linear regime: a microwave study," Phys. Rev. Lett. **104**, 093901 (2010).
9. S. Barkhofen, J. J. Metzger, R. Fleischmann, U. Kuhl, and H. J. Stöckmann, "Experimental observation of a fundamental length scale of waves in random media," Phys. Rev. Lett. **111**, 183902 (2013).
10. L. H. Ying, Z. Zhuang, E. J. Heller, and L. Kaplan, "Linear and nonlinear rogue wave statistics in the presence of random currents," Nonlinearity **24**, R67–R87 (2011).
11. H. Degueldre, J. J. Metzger, T. Geisel, and R. Fleischmann, "Random focusing of tsunami waves," Nat. Phys. **12**, 259–262 (2016).
12. A. Patsyk, U. Sivan, M. Segev, and M. A. Bandres, "Observation of branched flow of light," Nature **583**, 60–65 (2020).
13. J. J. Metzger, R. Fleischmann, and T. Geisel, "Statistics of extreme waves in random media," Phys. Rev. Lett. **112**, 203903 (2014).
14. R. Bekenstein, Y. Kabessa, Y. Sharabi, O. Tal, N. Engheta, G. Eisenstein, A. J. Agranat, and M. Segev, "Control of light by curved space in nanophotonic structures," Nat. Photonics **11**, 664–670 (2017).
15. M. Bartelmann, "Gravitational lensing," Class. Quantum Gravity **27**, 233001 (2010).

16. K. Y. Bliokh and F. Nori, "Relativistic Hall effect," Phys. Rev. Lett. **108**, 120403 (2012).
17. M. A. Oancea, J. Joudioux, I. Y. Dodin, D. E. Ruiz, C. F. Paganini, and L. Andersson, "Gravitational spin Hall effect of light," Phys. Rev. D **102**, 024075 (2020).
18. C. Xu, A. Abbas, and L.-G. Wang, "Generalization of Wolf effect of light on arbitrary two-dimensional surface of revolution," Opt. Express **26**, 33263–33277 (2018).
19. C. Xu, A. Abbas, L.-G. Wang, S.-Y. Zhu, and M. S. Zubairy, "Wolf effect of partially coherent light fields in two-dimensional curved space," Phys. Rev. A **97**, 063827 (2018).
20. C. Xu, I. Dana, L.-G. Wang, and P. Sebbah, "Light chaotic dynamics in the transformation from curved to flat surfaces," Proc. Natl. Acad. Sci. USA **119**, e2112052119 (2022).
21. J. Zhu, Y. Liu, Z. Liang, T. Chen, and J. Li, "Elastic waves in curved space: mimicking a wormhole," Phys. Rev. Lett. **121**, 234301 (2018).
22. S. Batz and U. Peschel, "Linear and nonlinear optics in curved space," Phys. Rev. A **78**, 043821 (2008).
23. W. F. Ding and Z. Y. Wang, "The hollow Gaussian beam propagation on curved surface based on matrix optics method," J. Opt. **23**, 095603 (2021).
24. W. Ding and Z. Wang, "Laser propagation in a Rindler accelerated reference frame based on matrix optics," Opt. Express **29**, 28631–28642 (2021).
25. L. C. Andrews, R. L. Phillips, C. Y. Hopen, and M. A. Al-Habash, "Theory of optical scintillation," J. Opt. Soc. Am. A **16**, 1417–1429 (1999).
26. S. Batz and U. Peschel, "Solitons in curved space of constant curvature," Phys. Rev. A **81**, 053806 (2010).
27. M. Padgett, "Droplets set light in a spin," Nature **461**, 600–601 (2009).
28. X. Chen, G. Xiao, X. Han, W. Xiong, H. Luo, and B. Yao, "Observation of spin and orbital rotation of red blood cell in dual-beam fibre-optic trap with transverse offset," J. Opt. **19**, 055612 (2017).
29. K. Jiang, T. W. Huang, R. Li, M. Y. Yu, H. B. Zhuo, S. Z. Wu, C. T. Zhou, and S. C. Ruan, "Branching of high-current relativistic electron beam in porous materials," Phys. Rev. Lett. **130**, 185001 (2023).
30. K. Jiang, T. W. Huang, C. N. Wu, M. Y. Yu, H. Zhang, S. Z. Wu, H. B. Zhuo, A. Pukhov, C. T. Zhou, and S. C. Ruan, "Nonlinear branched flow of intense laser light in randomly uneven media," Matter Radiat. Extremes **8**, 024402 (2023).
31. V. H. Schultheiss, S. Batz, and U. Peschel, "Hanbury Brown and Twiss measurements in curved space," Nat. Photonics **10**, 106–110 (2016).
32. W. Ding and Z. Wang, "'Classical' coherent state generated by curved surface," New J. Phys. **24**, 113002 (2022).
33. V. H. Schultheiss, S. Batz, A. Szameit, F. Dreisow, S. Nolte, A. Tünnermann, S. Longhi, and U. Peschel, "Optics in curved space," Phys. Rev. Lett. **105**, 143901 (2010).
34. J. J. Metzger, R. Fleischmann, and T. Geisel, "Universal statistics of branched flows," Phys. Rev. Lett. **105**, 020601 (2010).
35. A. V. Startsev and Y. Y. Stoilov, "On the nature of laser polariton tracks in soap films," Quantum Electron. **34**, 569–571 (2004).
36. J. Emile, O. Emile, and F. Casanova, "Light guiding properties of soap films," Europhys. Lett. **101**, 34005 (2013).
37. E. Kogan and M. Kaveh, "Statistics of fluctuations for two types of crossover: from the ballistic to diffusive regime and from the orthogonal to unitary ensemble," Phys. Rev. B **51**, 16400–16402 (1995).
38. A. Patsyk, Y. Sharabi, U. Sivan, and M. Segev, "Incoherent branched flow of light," Phys. Rev. X **12**, 021007 (2022).
39. Z. Shao and Z. Wang, "Propagation and transformation of a light beam on a curved surface," Opt. Express **29**, 8626–8634 (2021).
40. Y. Lamhot, A. Barak, C. Rotschild, M. Segev, M. Saraf, E. Lifshitz, A. Marmur, R. El-Ganainy, and D. N. Christodoulides, "Optical control of thermocapillary effects in complex nanofluids," Phys. Rev. Lett. **103**, 264503 (2009).
41. R. Schley, I. Kaminer, E. Greenfield, R. Bekenstein, Y. Lumer, and M. Segev, "Loss-proof self-accelerating beams and their use in non-paraxial manipulation of particles' trajectories," Nat. Commun. **5**, 5189 (2014).
42. S. Hod, "Bekenstein's generalized second law of thermodynamics: the role of the hoop conjecture," Phys. Lett. B **751**, 241–245 (2015).
43. N. A. Mortensen, "Air-clad fibers: pump absorption assisted by chaotic wave dynamics?" Opt. Express **15**, 8988–8996 (2007).
44. L. Philippe, V. Doya, R. Philippe, P. Dominique, M. Fabrice, and L. Olivier, "Experimental study of pump power absorption along rare-earth-doped double clad optical fibres," Opt. Commun. **218**, 249–254 (2003).